

Analysis of Phase and Amplitude Sensitivity for “300B” Bunch Compressor and Linac

Mike Church 4/12/06

Methodology:

The purpose of this analysis is to define tolerances for LLRF phase and amplitude signals for the bunch compressor and linac. Two criteria are considered here: 1) loss of luminosity due to collisions occurring away from the optimum collision point (timing jitter); and 2) increased energy spread at the IP (energy jitter). There is an additional criterion which should perhaps be considered also (eventually) – residual vertical dispersion at the IP. If there is residual dispersion at the IP, then energy jitter will cause the beams to shift vertically and not collide head on, thus contributing to loss of luminosity.

The lattice files used in these calculations were obtained from [Accelerator Development: G3 Bunch Compressor - ILC @ SLAC](#) on 12/20/05. The calculational tool being used for tracking is MAD8.23. The nominal ILC parameters are used for tracking through the linac, except the IP energy is 262 GeV. Except for the introduced phase and amplitude errors, there are no other introduced errors – the linac is otherwise “perfect.” Wakefields are turned off for these calculations. The inclusion of longitudinal wakefields will produce a slightly different longitudinal distribution at the IP, however variations of this distribution with respect to small variations in LLRF phase and amplitude are not significantly different whether wakefields are on or off. (The inclusion of wakefields slows the calculation down immensely.) The program Guinea Pig is used to calculate luminosity and luminosity vs. energy at the IP.

A distribution of 1000 particles is tracked from the the front of the bunch compressor to the end of the linac. (The longitudinal distribution does not change appreciably in travelling from the end of the linac to the IP.) The initial distribution is thrown gaussian in all dimensions with $\sigma_{ct}=6\text{mm}$, $\sigma_p/p=.15\%$. Transverse gaussian distributions are also included, with $\gamma\epsilon_x=10\text{E-}6$ and $\gamma\epsilon_y=4\text{E-}8$. Distributions are cut off at $\pm 3.9\sigma$. (The transverse distributions are irrelevant for this calculation.) Eight different error configurations are examined:

- 1) Correlated bunch compressor phase errors – all bunch compressor klystrons have the same phase error, and this error is distributed gaussian from pulse to pulse.
- 2) Uncorrelated bunch compressor phase errors – bunch compressor klystrons have uncorrelated phase errors, distributed gaussian.
- 3) Correlated bunch compressor amplitude errors – bunch compressor klystrons have correlated amplitude errors, and this error is distributed gaussian from pulse to pulse.
- 4) Uncorrelated bunch compressor amplitude errors – bunch compressor klystrons have uncorrelated amplitude errors, distributed gaussian.
- 5) Correlated linac phase errors – all linac klystrons have the same phase error, and this error is distributed gaussian from pulse to pulse.
- 6) Uncorrelated linac phase errors – linac klystrons have uncorrelated phase errors, distributed gaussian.
- 7) Correlated linac amplitude errors – linac klystrons have correlated amplitude errors, and this error is distributed gaussian from pulse to pulse.
- 8) Uncorrelated linac amplitude errors – linac klystrons have uncorrelated amplitude errors, distributed gaussian.

For each configuration, 5-10 data points are generated, with each data point consisting of a different error σ (independent variable), an average loss in luminosity (dependent variable), and an RMS width of center-of-mass energy at the IP (2nd dependent variable). Each data point is generated from tracking the ensemble of particles through 200 lattices with different error distribution seeds. This represents 100 collisions per data point. Errors in the electron and positron linacs are uncorrelated. All error distributions are cut off at $\pm 3.9\sigma$. The loss in luminosity is calculated from the IP position using the fit from Figure 4.

Results:

Because of the strong beam-beam effect at the IP, luminosity is not maximized when the collision point is located exactly at the waists of the final foci. Luminosity is maximized when the final foci are 230 μm upstream of the collision point. This is shown in Figures 1 and 2. All calculations in this paper are done in this optimized configuration. The luminosity vs. collision point jitter is shown in Figures 3 and 4. The fit to a 4th order polynomial gives.

$$dL/L(\%) = -0.00015487 \times z^2 + 1.6059 \times 10^{-10} \times z^4 \quad (z \text{ is IP offset in } \mu\text{m})$$

Figure 5 shows luminosity vs energy. The RMS of this distribution (cut off at ± 1 GeV) is 0.39 GeV. Figures 6-13 show the average luminosity loss and RMS width of the center-of-mass energy for each of the 8 error configurations. The lines in these plots are simply “connect-the-dots.” One can pick off the allowed tolerances from these plots. Table 1 shows a summary of phase and amplitude tolerances for each of the error configurations assuming 1) a 2% loss in luminosity is tolerable, and 2) a 10% increase in the RMS center-of-mass energy spread is tolerable. It is assumed that the energy spread from LLRF errors adds in quadrature with the “natural” (ie, due to beam width) energy spread, so that the 10% limit corresponds to an RMS width of $1.1 \times .39 \text{ GeV} = .43 \text{ GeV}$. I believe this means that the energy jitter is occurring on a time scale faster than the beam energy is being measured by downstream diagnostics. Perhaps this is a pessimistic assumption.

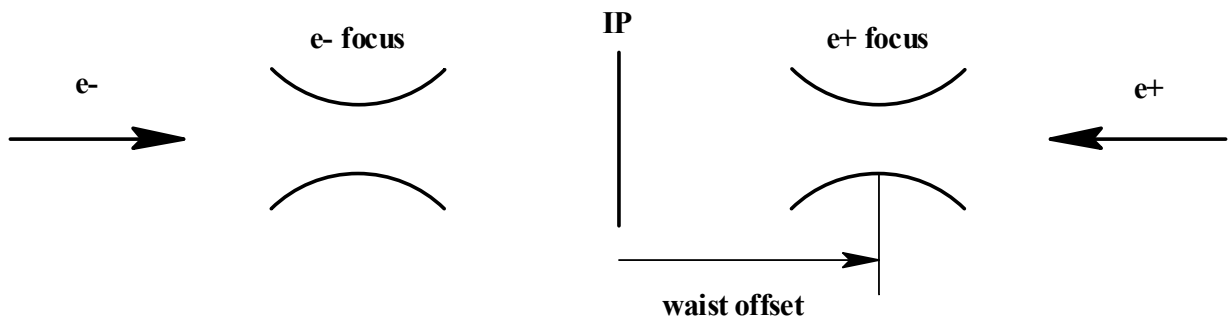


Figure 1: Arrangement of final focus waist and collision point.

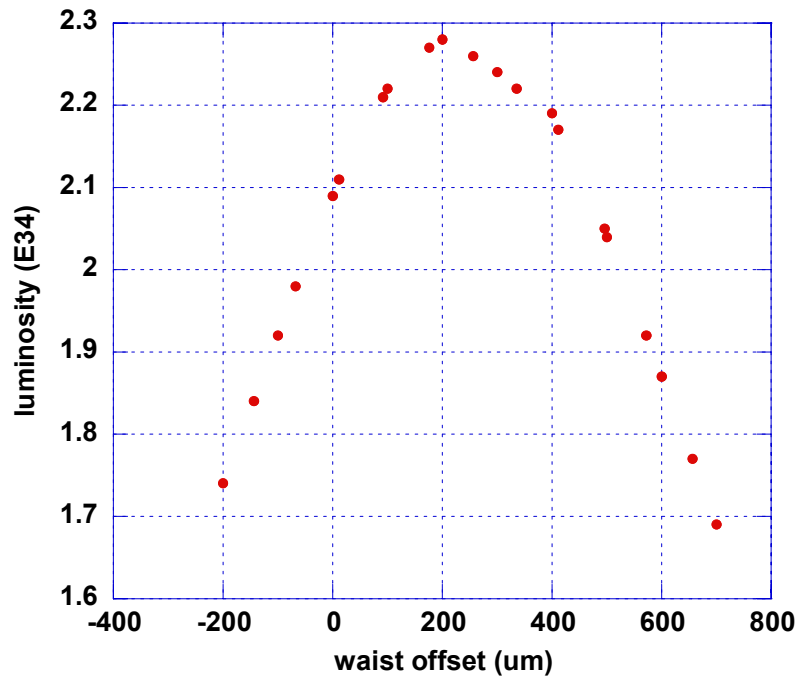


Figure 2: Luminosity vs. waist offset (ILC nominal)

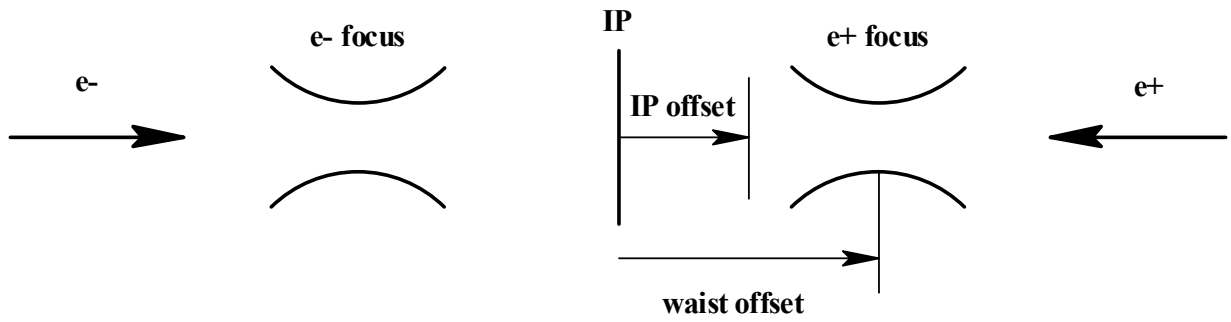


Figure 3: IP offset defines the time jitter of the collision point

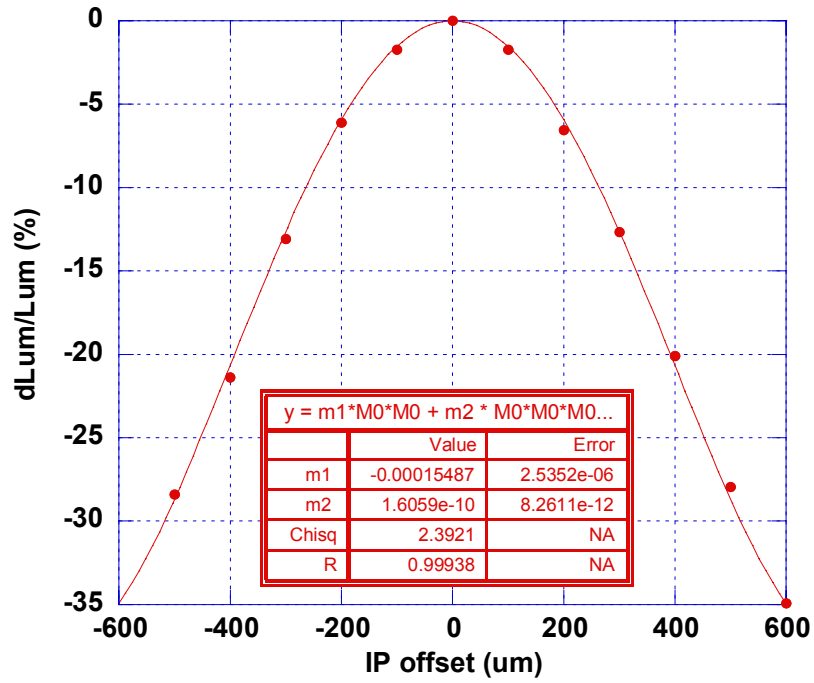


Figure 4: Luminosity vs IP offset (ILC nominal). The curve is a fit to a 4th order polynomial

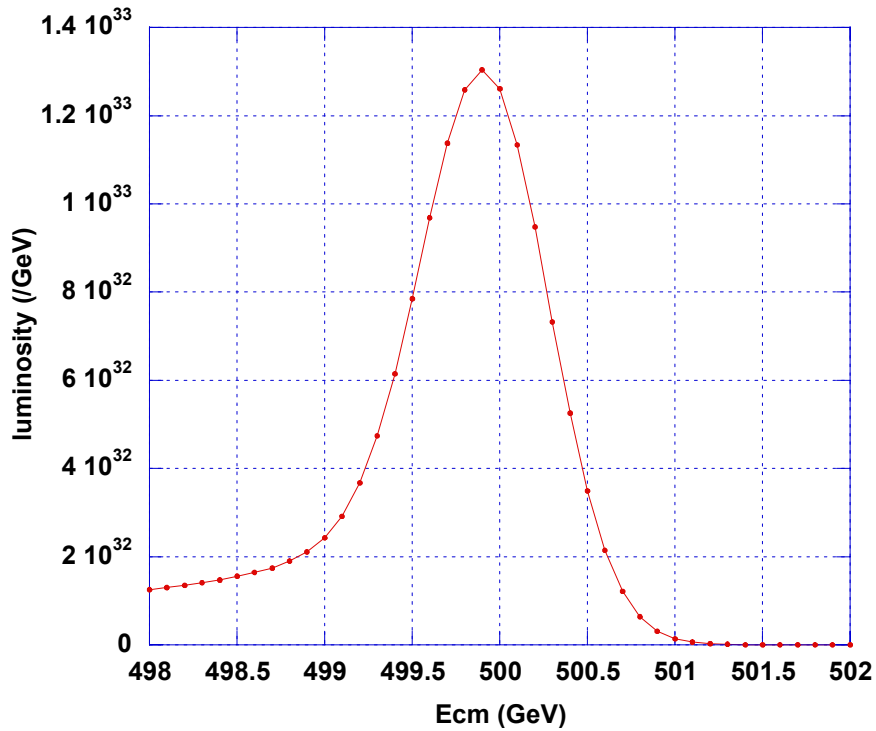


Figure 5: Luminosity vs energy (ILC nominal). RMS is 0.39GeV, cut at ± 1 GeV

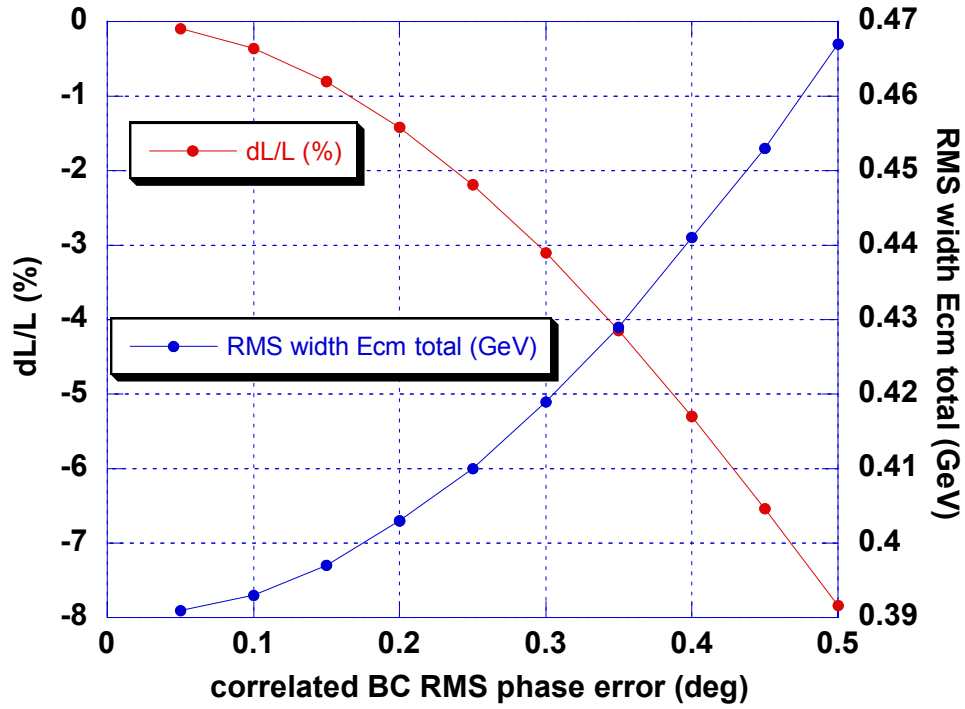


Figure 6: Luminosity loss and RMS width of center-of-mass energy for correlated bunch compressor phase errors

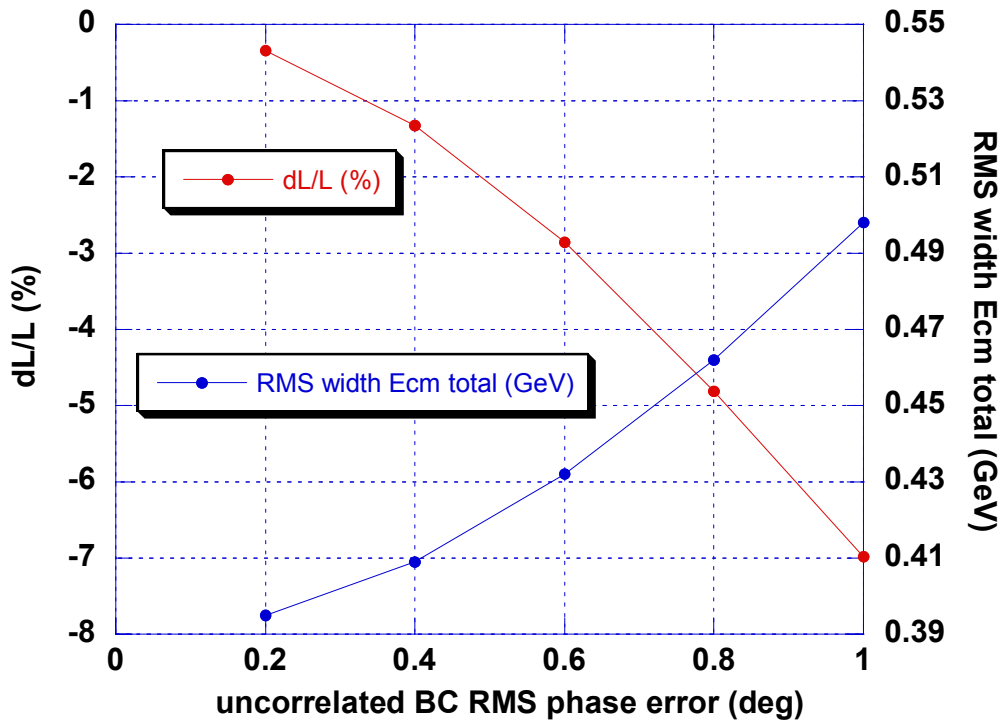


Figure 7: Luminosity loss and RMS width of center-of-mass energy for uncorrelated bunch compressor phase errors

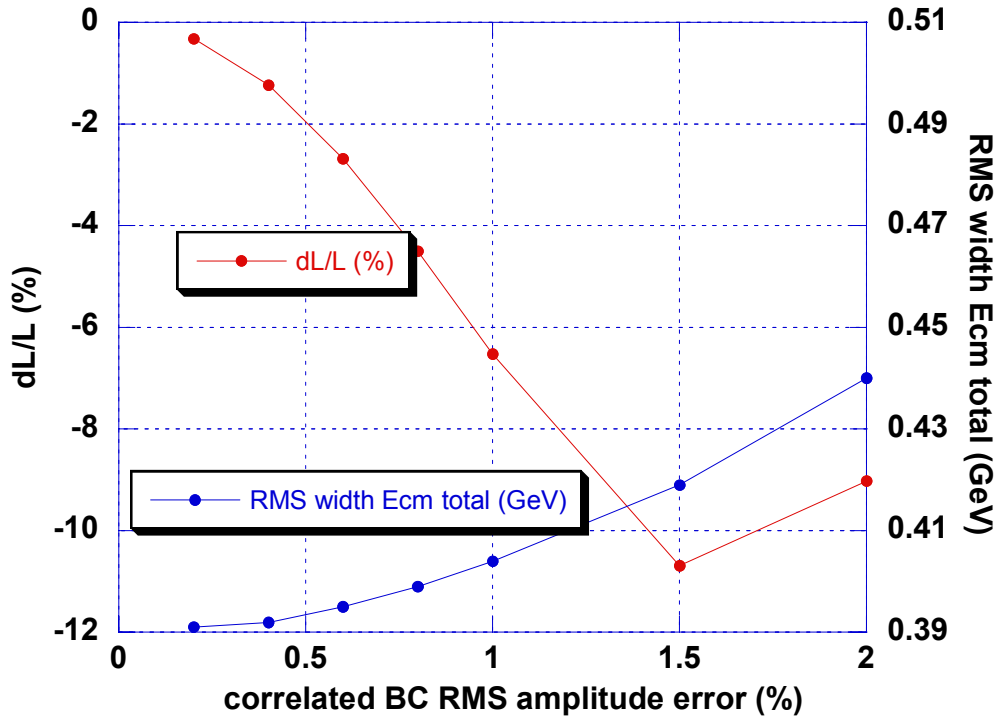


Figure 8: Luminosity loss and RMS width of center-of-mass energy for correlated bunch compressor amplitude errors

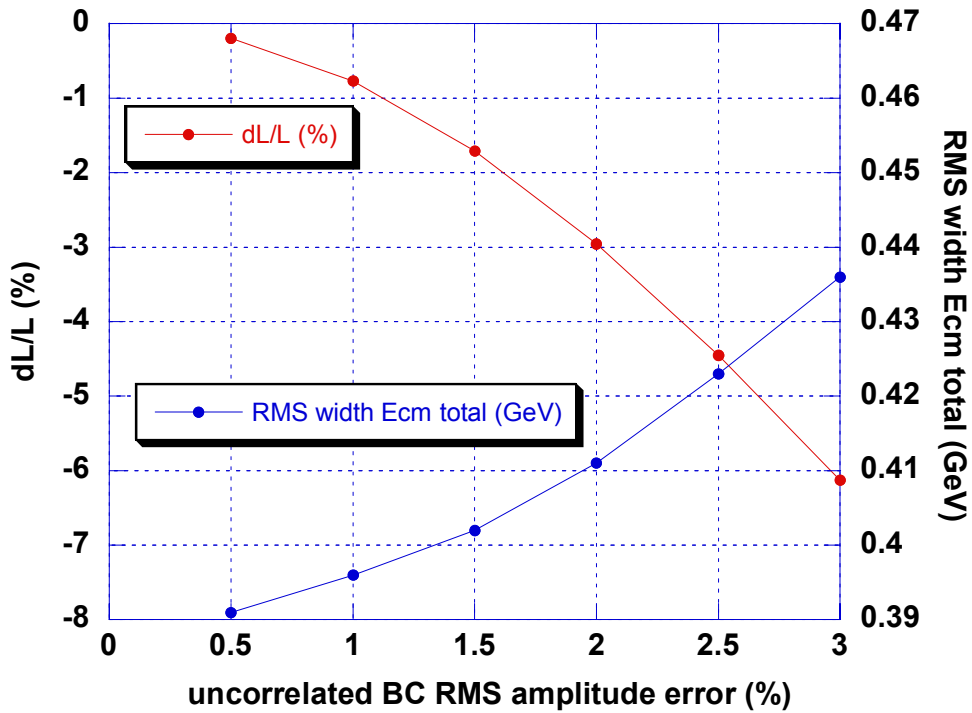


Figure 9: Luminosity loss and RMS width of center-of-mass energy for uncorrelated bunch compressor amplitude errors

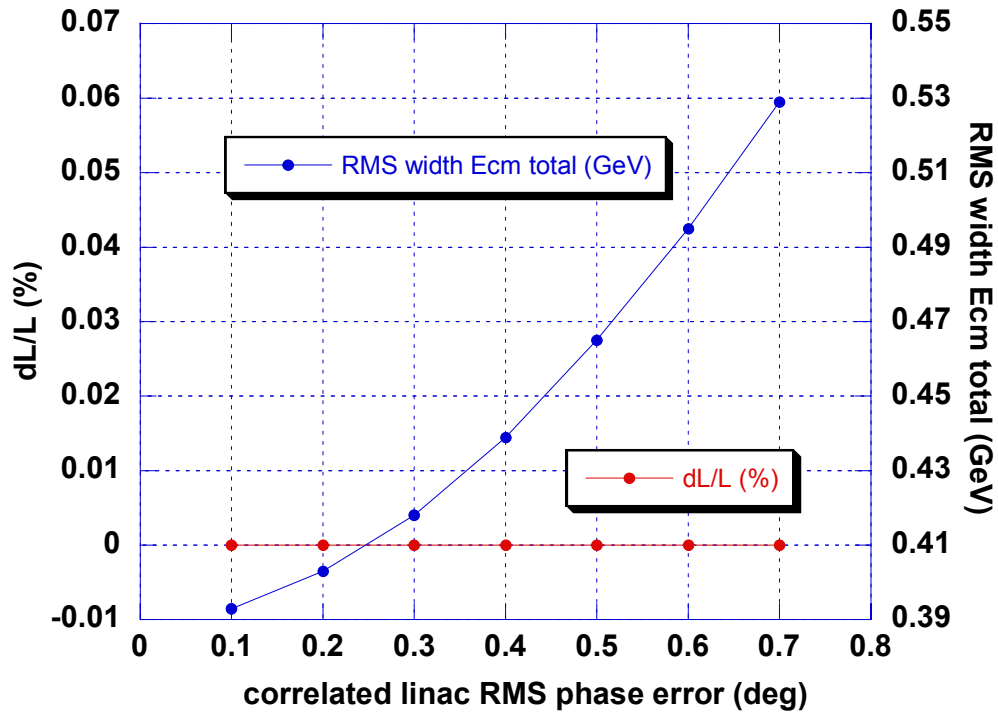


Figure 10: Luminosity loss and RMS width of center-of-mass energy for correlated linac phase errors

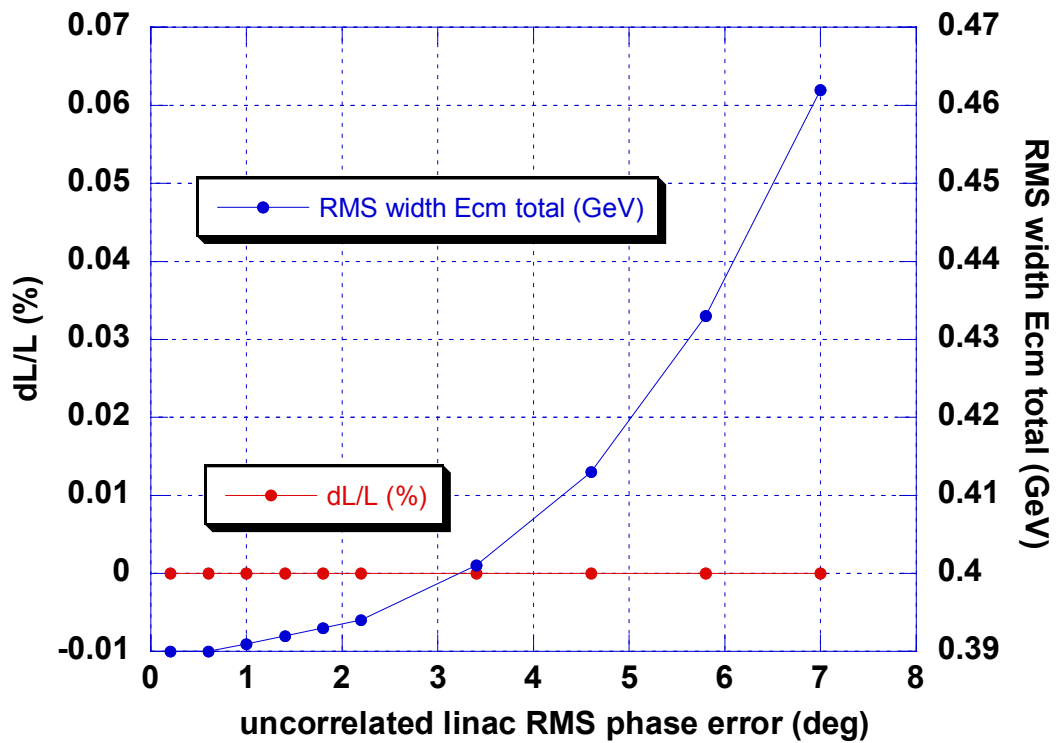


Figure 11: Luminosity loss and RMS width of center-of-mass energy for uncorrelated linac phase errors

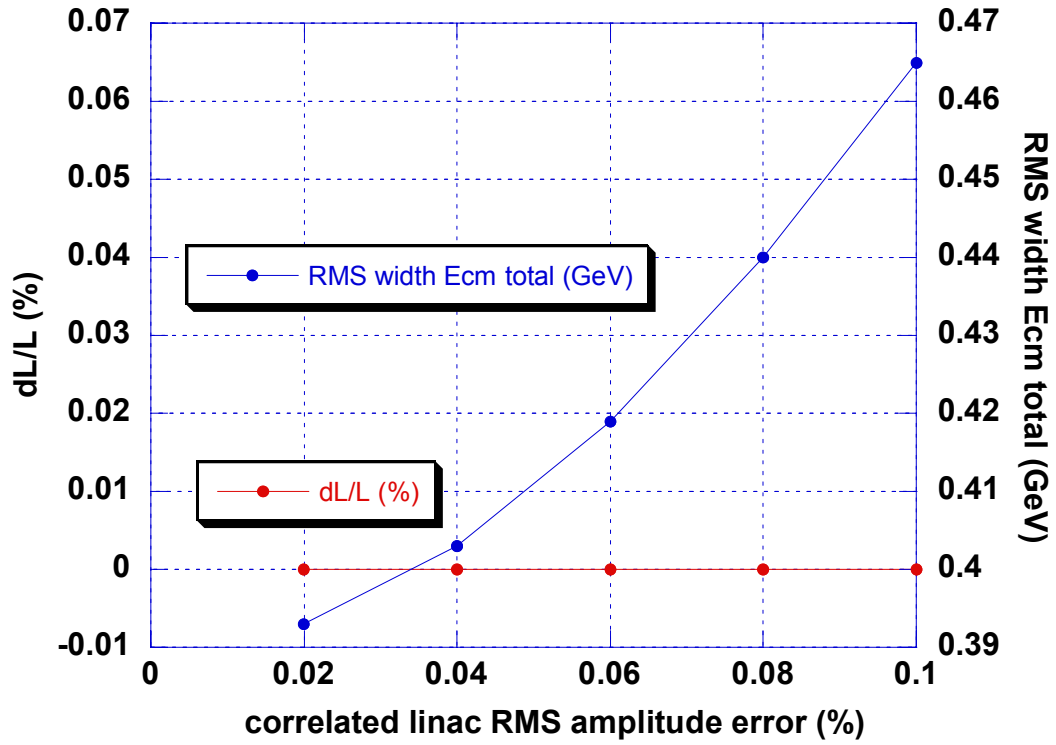


Figure 12: Luminosity loss and RMS width of center-of-mass energy for correlated linac amplitude errors

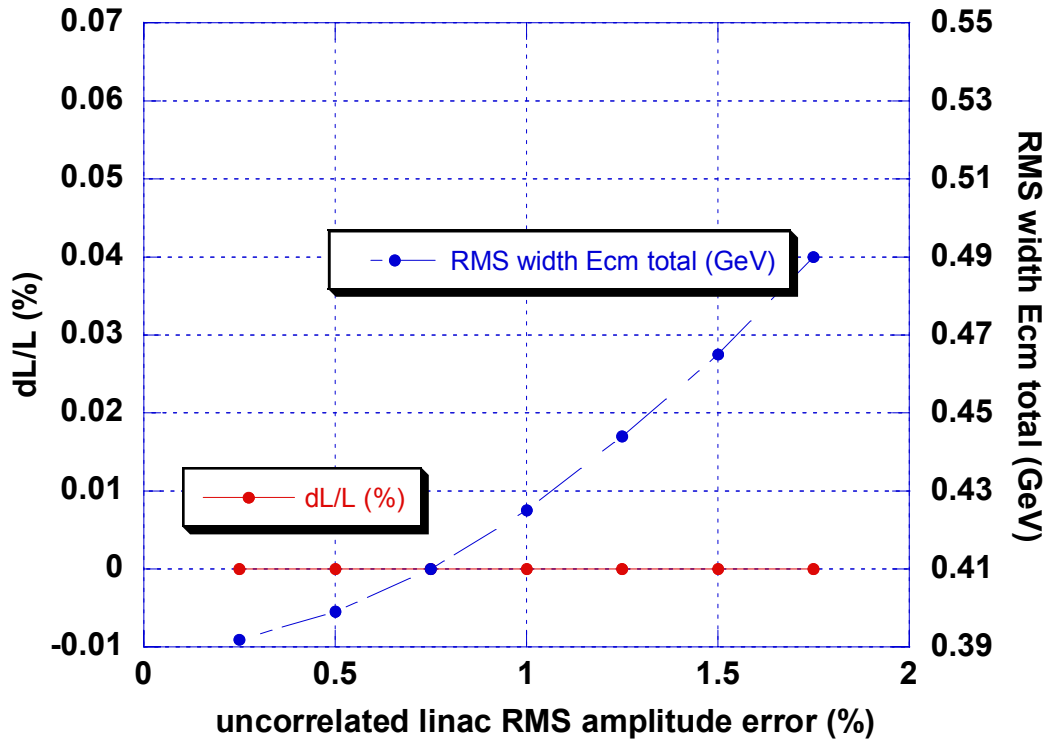


Figure 13: Luminosity loss and RMS width of center-of-mass energy for uncorrelated linac amplitude errors

	phase tolerance limiting luminosity loss (deg)	phase tolerance limiting increase in energy spread (deg)	amplitude tolerance limiting luminosity loss (%)	amplitude tolerance limiting increase in energy spread (%)
correlated BC phase errors	.24	.35		
uncorrelated BC phase errors	.48	.59		
correlated BC amplitude errors			0.5	1.8
uncorrelated BC amplitude errors			1.6	2.8
correlated linac phase errors	large	.36		
uncorrelated linac phase errors	large	5.6		
correlated linac amplitude errors			large	.07
uncorrelated linac amplitude errors			large	1.05

Table 1: Summary of tolerances for phase and amplitude control. These tolerances limit the average luminosity loss to <2% and limit the increase in RMS center-of-mass energy spread to <10% of the nominal energy spread.